Multi-delay arterial spin labeling brain magnetic resonance imaging study for pediatric autism

Tatsuo MORI[a*], Hiromichi ITO[a,b], Masafumi HARADA[c], Sonoka HISAOKA[c], Yuki MATSUMOTO[c], Aya GOJI[a], Yoshihiro TODA[a], Kenji MORI[a,d], Shoji KAGAMI[a]

[a]Department of Pediatrics, Institute of Biomedical Sciences, Tokushima University, Japan
[b]Department of Special Needs Education, Graduate School of Education, Naruto University of Education, Tokushima, Japan
[c]Department of Radiology, Institute of Biomedical Sciences, Tokushima University, Japan
[d]Department of Child Health & Nursing, Institute of Biomedical Sciences, Tokushima University Graduate School, Tokushima, Japan

***Corresponding author**:
Tatsuo Mori, M.D
Department of Pediatrics, Graduate School of Biomedical Sciences, Tokushima University, University of Tokushima
3-18-15 Kuramoto-cho, Tokushima 770-8503 Japan
Tel: +81-88-633-7135
Fax: +81-88-631-8697
E-mail: mori.tatsuo@tokushima-u.ac.jp

Abstract

Introduction

Arterial spin labeling (ASL) is a non-invasive magnetic resonance imaging (MRI) technique that can measure regional cerebral blood flow (rCBF) without radiation exposure. This study aimed to evaluate rCBF in individuals with autism and their age-matched controls, globally and regionally.

Methods

We performed ASL MRI (3T, pulsed-continuous ASL, 3 delayed ASL imaging sequences) for 33 patients with autism spectrum disorder (ASD) (average age: 7.3 years, range: 2-14 years). Nineteen children (average age: 8.6 years, range: 3-15 years) without ASD and intellectual delay were included as controls. Patients with morphological abnormalities detected on MRI were excluded. Objective analysis was performed with automatic region of interest analysis of the ASL results. The Mann-Whitney U test was used to compare the rCBF results between the groups.

Results

Compared to the controls, patients with ASD showed a statistically significant decrease in rCBF, respectively, in the insula [left, rCBF 51.8±9.5 mL/100 g/min (mean±SD) versus 59.9±9.8, p=0.0017; right, 51.2±10.1 versus 57.8±8.8, p=0.0354], superior parietal lobule (left, 44.6±8.4 versus 52.0±7.8, p=0.003), superior temporal gyrus (left, 50.0±8.6 versus 56.9±8.6, p=0.007; right, 49.5±8.4 versus 56.4±7.7, p=0.0058), and inferior frontal gyrus (left, 53.0±9.8 versus 59.3±9.9, p=0.0279), which are associated with the mirror neuron system.

Conclusions

We concluded that patients with ASD showed a statistically significant decline in CBF in regions associated with the mirror neuron system. The advantages of ASL MRI include low invasiveness (no radiation exposure) and short imaging time (approximately 5 min). Studies with larger sample sizes are required to establish the diagnostic value of ASL MRI for ASD.

Keywords: arterial spin labeling, autism spectrum disorder, cerebral blood flow,

magnetic resonance imaging, mirror neuron system

Introduction

It is thought that early detection and intervention contribute to good outcomes in social adaptation in patients with autism spectrum disorders (ASD) [1]. However, the diagnostic process depends on the physician's interview. The establishment of objective biomarkers (e.g., cerebral function, cerebral perfusion) for ASD may aid in the auxiliary diagnosis of ASD.

Functional magnetic resonance imaging (MRI) and near-infrared spectroscopy (NIRS) are useful for the examination of cerebral function [2,3]. However, these examinations involve the performance of tasks, which can be difficult for patients with developmental delay, who cannot easily follow the examiner's instructions. In contrast, regional cerebral blood flow (rCBF) single photon emission computed tomography (SPECT) does not require the performance of any tasks. Therefore, even patients with intellectual delays can undergo these investigations.

Hashimoto et al. demonstrated the decrease in frontal and temporal rCBF in the autistic brain, using CBF SPECT. The decrease in rCBF was more pronounced in patients with intellectual delay and those who were unable to use language, than in those without this disability [4]. Ohnishi et al. demonstrated that the insula, superior temporal gyrus, and prefrontal area showed a focal decrease in rCBF in young patients with ASD [5]. Further studies are needed, to establish a consensus, but the risk of radiation exposure discouraged patients with ASD and normal controls from participating in SPECT studies.

Arterial spin labeled (ASL) perfusion MRI permits noninvasive quantification of blood flow, an important physiological parameter [6]. This method involves labeling the proton spins of the inflowing water in arterial blood, by continuously inverting them at the neck region and observing the effects of this inversion on the intensity of the brain MRI. The increase in the use of 3T clinical MRI systems has dramatically improved the quality of ASL imaging, along with the development of ASL techniques. However, quantitative measurement of rCBF using ASL depends on several parameters, including T1 of brain tissue, T1 of arterial blood, and arterial transit time (ATT), which denotes the duration required by the labeled blood to travel from the labeling region to the imaged tissue. Transit time considerations are crucial in measuring absolute rCBF using ASL; thus, ASL methods using multiple post-label delay acquisitions were developed [7].

ASL is commonly used to improve the precision of 3T MRI in patients with

brain infarction and epilepsy, because of its noninvasiveness [8,9]. MRI is routinely performed in several patients with ASD, and ASL approximately requires 3 additional minutes. ASL studies for rCBF in patients with ASD have also been reported recently. Jann K et al. reported frontotemporal hyperperfusion and hypoperfusion in the dorsal anterior cingulate cortex in patients with ASD [10]. Yerys BE et al. reported hypoperfusion in the fusiform gyrus, bilaterally and in the right inferior temporal gyrus [11]. However, ASL is still being developed, and the software to analyze results objectively have not been sufficiently developed.

ASL has the potential to become a good diagnostic test for ASD. We hypothesized that a decrease in the rCBF on ASL would be observed in the regions associated with ASD. In this study, we evaluate the possibility of using ASL MRI to evaluate the biomarkers for ASD, using standardization of the brain form and automatic creation of the region of interest (ROI).

Methods

We recruited patients who were diagnosed with ASD according to DSM-V at the Tokushima University Hospital from June 2014 to September 2016. Thirty-three patients with ASD, with an average age of 7.3 years (range: 2-16 years), were recruited and evaluated using ASL MRI. We also recruited 19 children without ASD and intellectual delay, with an average age of 8.6 years (range: 3-15 years), as controls. Patients with morphological abnormalities detected on MRI were excluded from both groups. The study was approved by the Institutional Review Board and informed consent was obtained from the family members of all the children, after the purpose and risks of the study had been fully explained.

All imaging data were acquired using a 3T-MRI (Discovery 750, GE Healthcare, Waukesha, Wisconsin, U.S.A) with 16-channel head coils. Pseudocontinuous ASL, with three pulse-labeling-delays, was performed in this study. All perfusion and reference images were acquired with a 3-dimensional stack-of-spirals rapid acquisition with refocused echoes imaging sequence[12]. The imaging parameters were as follows: repetition time, 6797 ms; inversion time, 1000 ms; echo time, 11.2 ms; flip angle, 111 degrees; field of view, 240×240 mm; slice thickness, 4 mm; post labeling delay, 1.00,1.57,2.46 seconds; 6 arms with 600 samples; number of excitations, 1; and total scan

time, 5 min 36 s. Corrected CBF maps were subsequently calculated by the MRI scanner and used for evaluation.

We used the iNEUROSTAT++® (Nihon Medi-Physics Co Ltd, Tokyo, Japan) software to standardize the brain forms, and iSSP3.5_2tz® (Nihon Medi+Physics, Tokyo, Japan) to compare the ASL results between the ASD and control groups. The extracted cortical activity of the ASD group was compared to that of the control group, using a two-sample Student's *t*-test on a pixel-by-pixel basis. Calculated *t* values were converted to *Z* values, using a probability integral transformation. Following the use of iNEUROSTAT++® for the standardization of the brain forms, NEURO FLEXER® (Nihon Medi-Physics Co Ltd, Tokyo, Japan) was used for automatic ROI analysis. The analysis results were calculated by automatically segmenting the brain into 54 categories, based on the Talairach Atlas. (Figures 1 and 2)

The Mann-Whitney U test was used to compare the measured values of rCBF in each ROI of the ASD and control groups. We used the Wechsler Intelligence Scale for Children-IV to measure the intelligence quotient (IQ) scores of all participants. The correlation between measured values of rCBF and IQ scores was analyzed using linear regression. $p<0.05$ was considered as statistically significant, for all the analyses. All data were analyzed using GraphPad Prism 6® (GraphPad Software Inc, La Jolla, California, U.S.A).

Results

The results of the ASL analysis with iSSP3.5_2tz® are as shown in Figure 3. The results of the ASL analysis with NEURO FLEXER® are as shown in Table 1.

Compared to the control group, patients with ASD showed a statistically significant decrease in rCBF in the subcallosal gyrus (left, p=0.0012; right, p=0.0393), insula (left, p=0.0017; right, p=0.0354), left superior parietal lobule (p=0.003), superior temporal gyrus (left, p=0.007; right, p=0.0058), transverse temporal gyrus (left, p=0.0099; right, p=0.014), left caudate (p=0.0112), left precentral gyrus (p=0.0144), supramarginal gyrus (left, p=0.0389; right, p=0.0146), middle temporal gyrus (left p=0.0252, right p=0.0496), uncus (left p=0.034, right p=0.0255), left inferior frontal gyrus (p=0.0279), right inferior temporal gyrus (p=0.0308), left inferior parietal lobule (p=0.0357), left anterior cingulate gyrus (p=0.0374), left postcentral gyrus (p=0.0432), and left lentiform

nucleus (p=0.0474) (Figures 4, 5, and 6), on analysis with NEURO FLEXER®.

Moreover, we further subdivided the two groups by age. Patients with ASD were subdivided into the 0-9 years subgroup [25 patients, average age :5.4 years (range: 2-9 years)] and the ≥10 years subgroup [8 patients, average age: 13.1 years (range: 10-16 years)]. The control group was also subdivided into the 0-9 years subgroup [11 children, 6.2 years (range: 3-9 years)] and the ≥ 10 years subgroup [8 children, 12.0 years (range: 10-15 years)]. As a result, a significant difference was discovered only in the left insula in the 0-9 years subgroup [rCBF 50.0±7.6 (mean±SD) of ASD versus 56.4±11.0 in control, p=0.0452], and left superior parietal lobule in the ≥10 years subgroup (43.4±7.2 versus 55.0±6.3, p=0.0047).

We evaluated the correlation between IQ scores and the ASL MRI results for the bilateral insulae, superior temporal gyri, and inferior frontal gyri using linear regression; however, no statistically significant correlation was observed (Figure 7).

Discussion

This study found a statistically significant reduction in the blood flow to the insula, superior temporal gyrus, left inferior frontal gyrus, and left inferior parietal lobule using ASL MRI. These areas are closely associated with the mirror neuron system and the theory of the mind, which are often impaired in children with ASD.

It has recently been proposed that dysfunction of the mirror neuron system during early development could cause a cascade of impairments that are characteristic of ASD, including deficits in imitation, theory of mind, and social communication [13]. This system is thought to provide a neural mechanism by which others' actions and intentions can be automatically understood [14].

Some human brain regions such as the lower frontal gyrus, inferior parietal lobule, and premotor area are also considered as part of the mirror-neuron system, based on functional MRI studies [15]. The visuoperceptual characteristics of the movements of others are analyzed in the superior temporal gyrus. This information is conveyed to the mirror neuron system [16]. Furthermore, this cortical system is linked to the limbic system by the anterior sector of the insular lobe [17].

Moreover, our study found a statistically significant reduction in blood flow to the subcallosal gyrus. The subcallosal gyrus sends projections to the amygdala and is involved in the suppression of the amygdala's responsiveness to fear-inducing cues. Dysfunction of this area may be responsible for the failure of extinction of the fear response, which is an important part of the anxiety response [18]. This dysfunction of the subcallosal gyrus may be related to anxiety, which several patients with ASD patients are likely to experience.

Our study also found a statistically significant reduction of blood flow to the uncus. The uncus of the hippocampus is the anterior-most portion of the medial parahippocampal gyrus and belongs to the limbic system. It is also a part of the olfactory system. It houses the primary olfactory cortex and receives fibers from the olfactory tract via the lateral olfactory stria [19]. Decreased blood flow to the uncus may be related to the olfactory and limbic abnormalities in ASD.

Furthermore, our study found a statistically significant reduction of blood flow to the transverse temporal gyrus. This structure (also called Heschl's gyrus) is a part of the primary auditory cortex [20]. Reduced blood flow to this region may be correlated with difficulties that autistic children experience, while processing auditory stimuli, compared to visual stimuli.

We also analyzed the rCBF in segmentalized age-groups. A significant difference was observed only in the left insula in the 0-9 years group and the left superior parietal lobule in the ≥10 years group. This result reflects the fact that it becomes difficult to determine a significant difference if the size of the sample is too small. However, these regions are associated with the mirror neuron system, thus reinforcing our results.

Finally, the lack of correlation between the IQ scores and measured decrease in rCBF suggests that the difficulty experienced by patients with ASD in daily life is not necessarily correlated with their IQ.

The present study has some limitations. First, some children in the control group showed reduction of rCBF in the ROI related to the mirror neuron system. Therefore, we were unable to diagnose ASD by ASL MRI alone. Correlation of the results of diffusor tensor imaging/functional MRI with rCBF results obtained by ASL could have aided the diagnosis. Second, an autism assessment tool such as the Parent-interview ASD Rating Scale-Text Revision should have been used, to better evaluate the relationship between ASD characteristics and rCBF. Third, the site of the hypoperfusion reported by

previous ASL study in patients with ASD [9,10] were different from our study. However, several points are similar to the SPECT study, including hypoperfusion in the regions associated with the mirror neuron system [4,5].

Conclusion

In this study, ASL MRI demonstrated a statistically significant decline in rCBF in regions associated with the mirror neuron system in patients with ASD. ASL MRI had potential as a useful diagnostic technique for ASD. ASL MRI is highly advantageous, owing to its noninvasiveness (no radiation exposure) and short imaging time (approximately 5 min). However, the sample size of our study was small. Further studies with larger sample sizes are required, to irrefutably establish the diagnostic value of ASL MRI. It is also necessary to evaluate the correlation between the severity of ASD and the reduction in rCBF measured by ASL MRI, using autism assessment scales such as the Parent-interview ASD Rating Scale-Text Revision.

Declaration of Competing Interests

The authors declared no potential conflicts of interest with respect to the research, authorship, and/or publication of this article.

References

1. Dawson G, Rogers S, Munson J, Smith M, Winter J, Greenson J, et al. Randomized, controlled trial of an intervention for toddlers with autism: the Early Start Denver Model. Pediatrics 2010;125:e17–23.
2. Wang AT, Lee SS, Sigman M, Dapretto M. Reading Affect in the Face and Voice: Neural Correlates of Interpreting Communicative Intent in Children and Adolescents with Autism Spectrum Disorders. Arch Gen Psychiatry 2007;64:698–708.
3. Mori K, Toda Y, Ito H, Mori T, Mori K, Goji A, et al. Neuroimaging in autism spectrum disorders: 1H-MRS and NIRS study. J Med Invest 2015;62:29–36.
4. Hashimoto T, Sasaki M, Fukumizu M, Hanaoka S, Sugai K, Matsuda H. Single-photon emission computed tomography of the brain in autism: effect of the developmental level. Pediatr Neurol 2000;23:416–20.
5. Ohnishi T, Matsuda H, Hashimoto T, Kunihiro T, Nishikawa M, Uema T, et al. Abnormal regional cerebral blood flow in childhood autism. Brain 2000;123:1838–44.
6. Alsop DC, Detre JA, Golay X, Günther M, Hendrikse J, Hernandez-Garcia L, et al. Recommended implementation of arterial spin-labeled perfusion MRI for clinical applications: A consensus of the ISMRM perfusion study group and the European consortium for ASL in dementia. Magn Reson Med 2015;73:102-16.
7. Tsujikawa T, Kimura H, Matsuda T, Fujiwara Y, Isozaki M, Kikuta K, et al. Arterial Transit Time Mapping Obtained by Pulsed Continuous 3D ASL Imaging with Multiple Post-Label Delay Acquisitions: Comparative Study with PET-CBF in Patients with Chronic Occlusive Cerebrovascular Disease. PLoS One 2016;11:e0159894.
8. Okazaki S, Yamagami H, Yoshimoto T, Morita Y, Yamamoto H, Toyoda K, et al. Cerebral hyperperfusion on arterial spin labeling MRI after reperfusion therapy is related to hemorrhagic transformation. J Cereb Blood Flow Metab 2017;37:3087–90.
9. Ho ML. Arterial spin labeling: Clinical applications. J Neuroradiol 2018;45:276–89.
10. Jann K, Hernandez LM, Beck-Pancer D, McCarron R, Smith RX, Dapretto M, et al. Altered resting perfusion and functional connectivity of default mode network in youth with autism spectrum disorder. Brain Behav 2015;5:e00358.

11. Yerys BE, Herrington JD, Bartley GK, Liu HS, Detre JA, Schultz RT. Arterial spin labeling provides a reliable neurobiological marker of autism spectrum disorder. J Neurodev Disord 2018;10:32.
12. Dai W, Shankaranarayanan A, Alsop DC. Volumetric measurement of perfusion and arterial transit delay using hadamard encoded continuous arterial spin labeling. Magn Reson Med. 2013;69:1014-22.
13. Dapretto M, Davies MS, Pfeifer JH, Scott AA, Sigman M, Bookheimer SY, et al. Understanding emotions in others: mirror neuron dysfunction in children with autism spectrum disorders. Nat Neurosci 2006;9:28–30.
14. Rizzolatti G, Craighero L. The mirror-neuron system. Annu Rev Neurosci 2004;27:169–92.
15. Iacoboni M, Woods RP, Brass M, Bekkering H, Mazziotta JC, Rizzolatti G. Cortical mechanisms of human imitation. Science 1999;286:2526–8.
16. Binkofski F, Buccino G, Posse S, Seitz RJ, Rizzolatti G, Freund H. A fronto-parietal circuit for object manipulation in man: evidence from an fMRI-study. Eur J Neurosci 1999 11:3276–86.
17. Hoffman M. How automatic and representational is empathy, and why. Behav Brain Sci 2002;25:38-9.
18. Vermetten E, Lanius RA. Biological and clinical framework for posttraumatic stress disorder. Handb Clin Neurol 2012;106:291–342.
19. Radiopaedia.org[Internet]. Uncus. [cited 2019 Jun 5]. Available from: https://radiopaedia.org/articles/uncus.
20. Amunts K, Morosan P, Hilbig H, Zilles K. Auditory System. In: Juergen Mai, George Paxinos, editors. The Human Nervous System (Third Edition) Cambridge: Academic Press Inc; 2012. p.1270-94.

Figure legends

Figure 1
Regions of interest (ROI) as seen on Neuro Flexer®.
The results of the analysis can be calculated, by automatically segmenting the brain into 54 categories, based on the Talairach Atlas, with the Level 3 setting of this software. The numbers are the same as in Figure 2.

Figure 2
Results of Neuro Flexer ® analysis for an 8-year-old boy in the control group and an 8-year-old boy in the ASD group.
ASD: autism spectrum disorder

Figure 3
Comparison of the ASL results between the ASD and control groups, as seen on iSSP3.5_2tz®.

ASL: arterial spin labeling. ASD: autism spectrum disorder

Figure 4
Statistically significant blood flow reduction detected by arterial spin labeling magnetic resonance imaging of the insula (left p=0.0017), superior temporal gyrus (left p=0.007), inferior frontal gyrus (left p=0.028), and inferior parietal lobule (left p=0.036) These areas are closely associated with the mirror neuron system and the theory of the mind, which are often impaired in children with autism spectrum disorders. These regions are essential for sympathy and for understanding others' intentions.

Figure 5
Statistically significant blood flow reduction detected by arterial spin labeling magnetic resonance imaging in the subcallosal gyrus (left, p=0.0012; right, p=0.039) The subcallosal gyrus sends projections to the amygdala and is involved in the suppression of the amygdala’s responsiveness to fear-inducing cues.

Figure 6
Statistically significant blood flow reduction detected by arterial spin labeling magnetic resonance imaging in the uncus (left, p=0.034; right, p=0.026) The uncus of the hippocampus is a part of the limbic and olfactory systems. Decreased blood flow to the uncus of the hippocampus may be related to the olfactory and limbic abnormalities seen in ASD.
ASD: autism spectrum disorder

Figure 7
Linear regression analysis showing a lack of statistically significant correlation between IQ scores and arterial spin labeling magnetic resonance imaging results for the bilateral insulae, superior temporal gyri, and inferior frontal gyri
IQ: intelligence quotient

Region of interest		ASD group (mean±SD)	Control group (mean±SD)	P value
Subcallosal Gyrus	Left	46.5±8.8	56.5±11.2	**0.0012
	Right	46.3±9.8	51.9±9.5	*0.039
Insula	Left	51.8±9.5	59.9±9.8	**0.0017
	Right	51.2±10.1	57.8±8.8	*0.035
Superior Parietal Lobule	Left	44.6±8.4	52.0±7.8	**0.003
Superior Temporal Gyrus	Left	50.0±8.6	56.9±8.6	**0.007
	Right	49.5±8.4	56.4±7.7	**0.0058
Transverse Temporal Gyrus	Left	52.5±10.0	59.8±9.9	**0.0099
	Right	49.7±9.9	56.5±8.3	**0.014
Caudate Gyrus	Left	42.8±7.3	48.2±6.8	*0.011
Precentral Gyrus	Left	51.9±10.1	58.5±8.5	*0.014
Supramarginal Gyrus	Left	53.6±10.6	60.8±10.9	*0.039
	Right	53.5±9.6	60.6±10.1	*0.015
Middle Temporal Gyrus	Left	51.7±9.2	58.1±9.6	*0.025
	Right	51.1±8.8	56.8±9.0	*0.0496
Uncus	Left	37.2±7.0	42.4±8.1	*0.034
	Right	37.1±6.0	42.6±8.4	*0.026
Inferior Frontal Gyrus	Left	53.0±9.8	59.3±9.9	*0.028
Inferior Temporal Gyrus	Right	46.8±7.9	52.9±8.7	*0.031
Inferior Parietal Lobule	Left	51.5±9.9	57.6±9.3	*0.036
Anterior Cingulate Gyrus	Left	50.7±9.4	57.0±10.0	*0.037
Postcentral Gyrus	Left	50.4±9.4	55.7±7.9	*0.043
Lentiform Nucleus	Left	42.0±6.8	45.8±7.9	*0.047

* $p<0.05$

** $p < 0.01$

Table 1

Sites with statistically significant decline in cerebral blood flow (detected by arterial spin labeling magnetic resonance imaging)

Figure 1

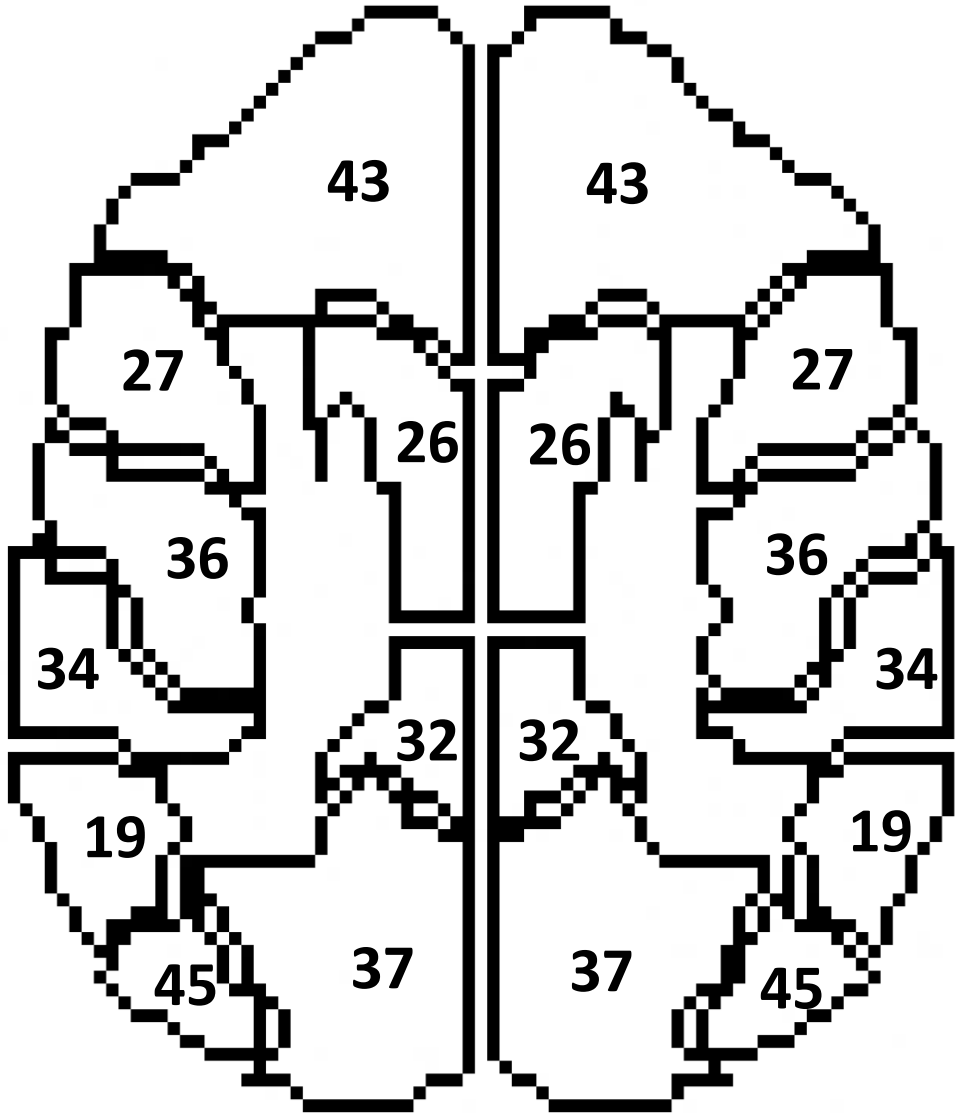

19	Inferior Parietal Lobule
26	Medial Frontal Gyrus
27	Middle Frontal Gyrus
32	Paracentral Lobule
34	Postcentral Gyrus
36	Precentral Gyrus
37	Precuneus
43	Superior Frontal Gyrus
45	Superior Parietal Lobule

Figure 2

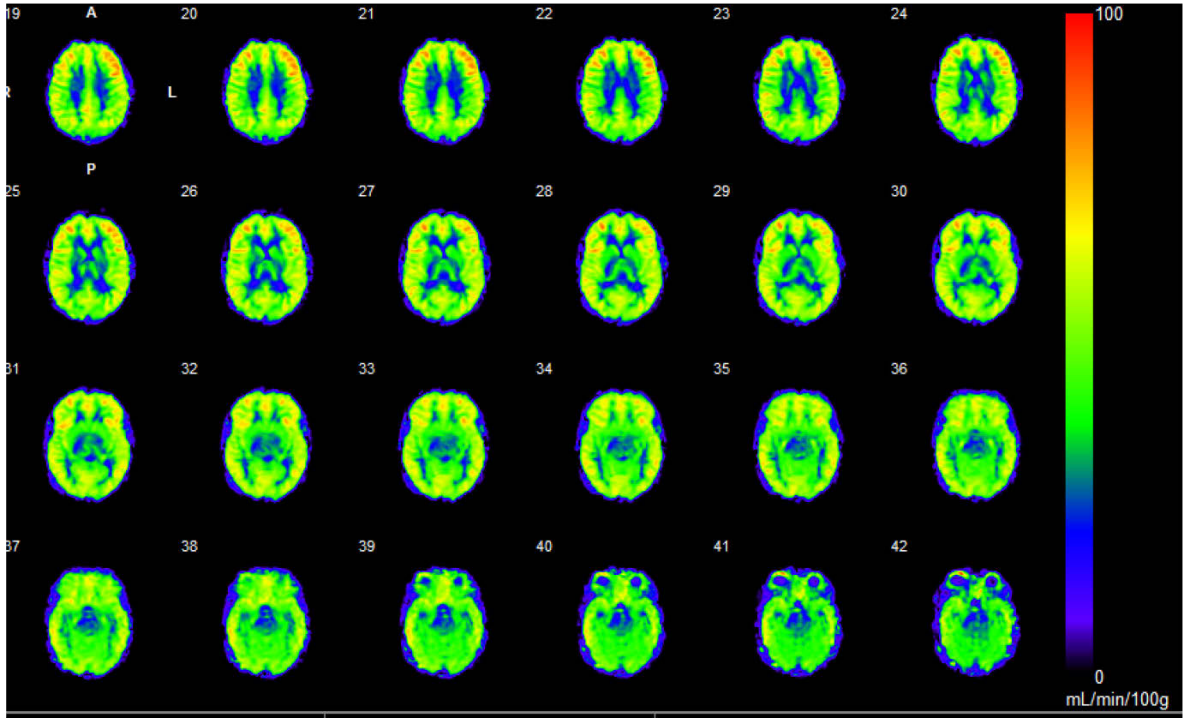

Territory	Right	Left	Territory	Right	Left	Territory	Right	Left
Anterior	40.09	39.16	Lv3_16	45.81	43.84	Lv3_34	52.34	53.16
Frontal	54.10	54.87	Lv3_17	55.31	55.69	Lv3_35	49.40	45.19
LimbicLobe	46.41	44.60	Lv3_18	51.96	48.57	Lv3_36	54.42	57.43
Midbrain		30.27	Lv3_19	55.67	52.15	Lv3_37	54.33	52.25
Occipital	50.97	49.46	Lv3_20	33.99	32.32	Lv3_38	35.16	34.00
Parietal	54.00	52.22	Lv3_21	49.87	49.23	Lv3_40	32.34	41.52
Pons		32.35	Lv3_22	54.50	52.62	Lv3_41	47.10	45.06
Posterior	37.66	36.86	Lv3_24	38.75	39.17	Lv3_43	53.35	52.79
Temporal	50.57	49.91	Lv3_25	52.56	48.35	Lv3_44	47.58	50.91
Lv3_01	54.28	55.19	Lv3_26	54.48	50.02	Lv3_45	52.07	47.10
Lv3_02	50.94	49.10	Lv3_27	56.91	61.43	Lv3_46	51.58	50.94
Lv3_03	41.30	42.12	Lv3_28	52.56	53.99	Lv3_47	55.21	54.93
Lv3_05	35.57	35.09	Lv3_29	54.89	55.17	Lv3_48	32.15	33.41
Lv3_06	50.89	49.64	Lv3_30	38.33	38.08	Lv3_50	53.82	53.11
Lv3_08	41.16	40.35	Lv3_31	26.63	37.72	Lv3_51	34.64	33.83
Lv3_10	49.55	48.21	Lv3_32	53.52	50.33	Lv3_53	37.56	36.92
Lv3_11	43.37	42.61	Lv3_33	38.76	37.47	Lv3_54	36.92	36.37

An 8-year-old-boy with ASD

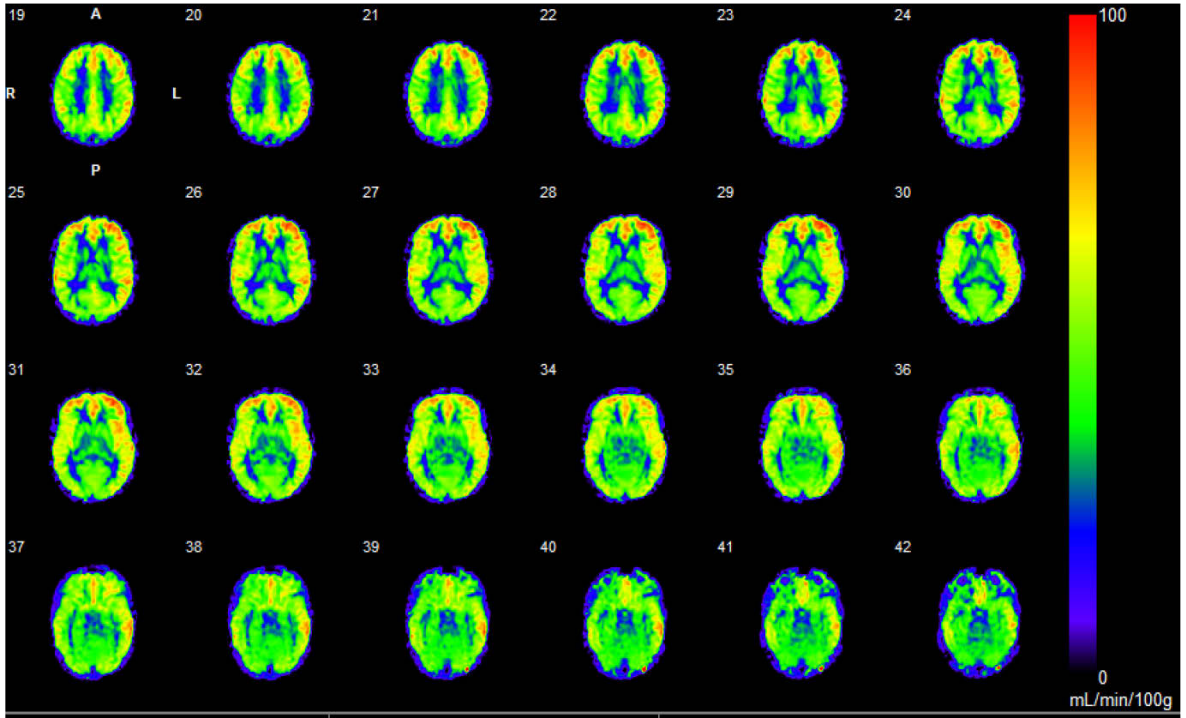

Territory	Right	Left	Territory	Right	Left	Territory	Right	Left
Anterior	36.87	37.18	Lv3_16	45.10	46.56	Lv3_34	52.19	52.73
Frontal	52.50	57.77	Lv3_17	52.89	56.64	Lv3_35	49.79	52.51
LimbicLobe	48.27	48.93	Lv3_18	50.42	54.21	Lv3_36	51.18	56.55
Midbrain		31.42	Lv3_19	54.23	58.52	Lv3_37	48.88	52.35
Occipital	46.49	50.74	Lv3_20	37.94	38.27	Lv3_38	35.44	39.64
Parietal	50.82	54.30	Lv3_21	49.28	56.66	Lv3_40	47.56	53.04
Pons		31.09	Lv3_22	56.42	61.76	Lv3_41	51.60	54.95
Posterior	37.14	38.52	Lv3_24	41.33	42.45	Lv3_43	53.50	58.60
Temporal	49.59	55.96	Lv3_25	43.53	47.36	Lv3_44	50.77	52.73
Lv3_01	51.61	59.08	Lv3_26	52.99	57.13	Lv3_45	45.38	53.25
Lv3_02	54.00	55.52	Lv3_27	55.89	62.49	Lv3_46	52.45	59.12
Lv3_03	41.02	43.52	Lv3_28	51.70	54.35	Lv3_47	53.15	62.58
Lv3_05	35.87	36.41	Lv3_29	51.08	59.37	Lv3_48	35.28	36.21
Lv3_06	53.58	54.99	Lv3_30	36.33	34.37	Lv3_50	57.43	63.23
Lv3_08	38.15	38.73	Lv3_31	31.45	36.45	Lv3_51	33.80	32.73
Lv3_10	44.54	50.74	Lv3_32	49.51	47.70	Lv3_53	38.51	42.19
Lv3_11	39.44	41.67	Lv3_33	40.29	37.34	Lv3_54	38.06	39.83

A normal 8-year-old-boy

Figure 3

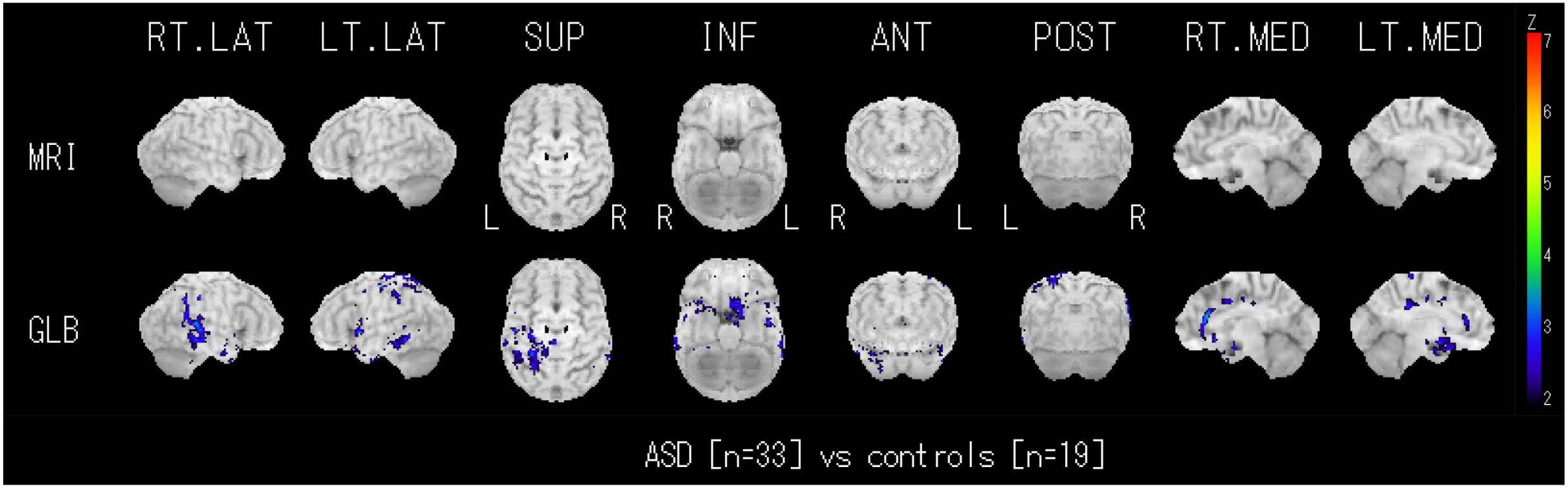
RT.LAT
LT.LAT
SUP
INF
ANT
POST
RT.MED
LT.MED
MRI
GLB
L
R
R
L
R
L
L
R
Z
7
6
5
4
3
2
ASD [n=33] vs controls [n=19]

Figure 4

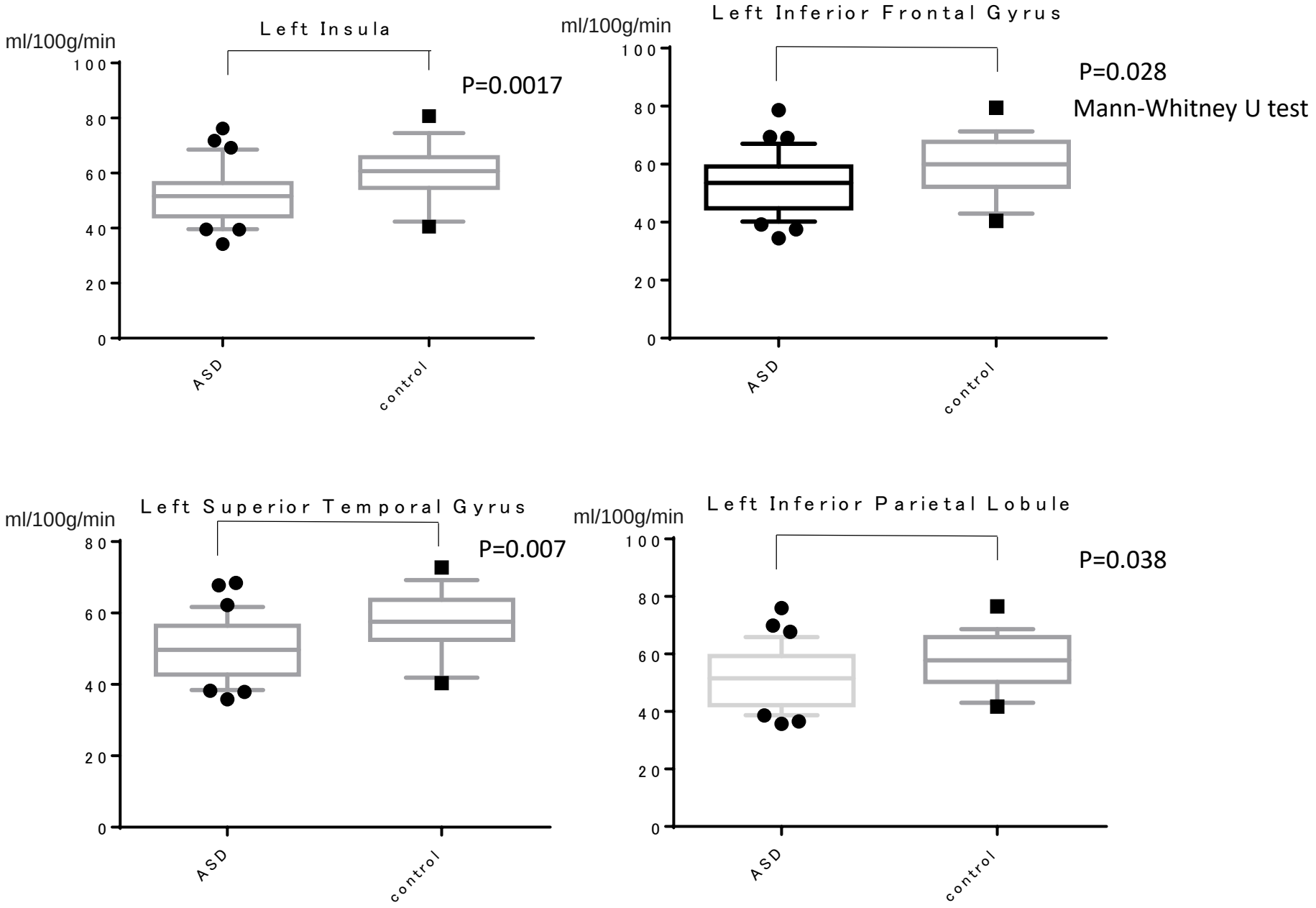
Left Insula
ml/100g/min
100
80
60
40
20
0
P=0.0017
ASD
control
Left Inferior Frontal Gyrus
ml/100g/min
P=0.028
Mann-Whitney U test
Left Superior Temporal Gyrus
ml/100g/min
P=0.007
Left Inferior Parietal Lobule
ml/100g/min
P=0.038

Figure 5

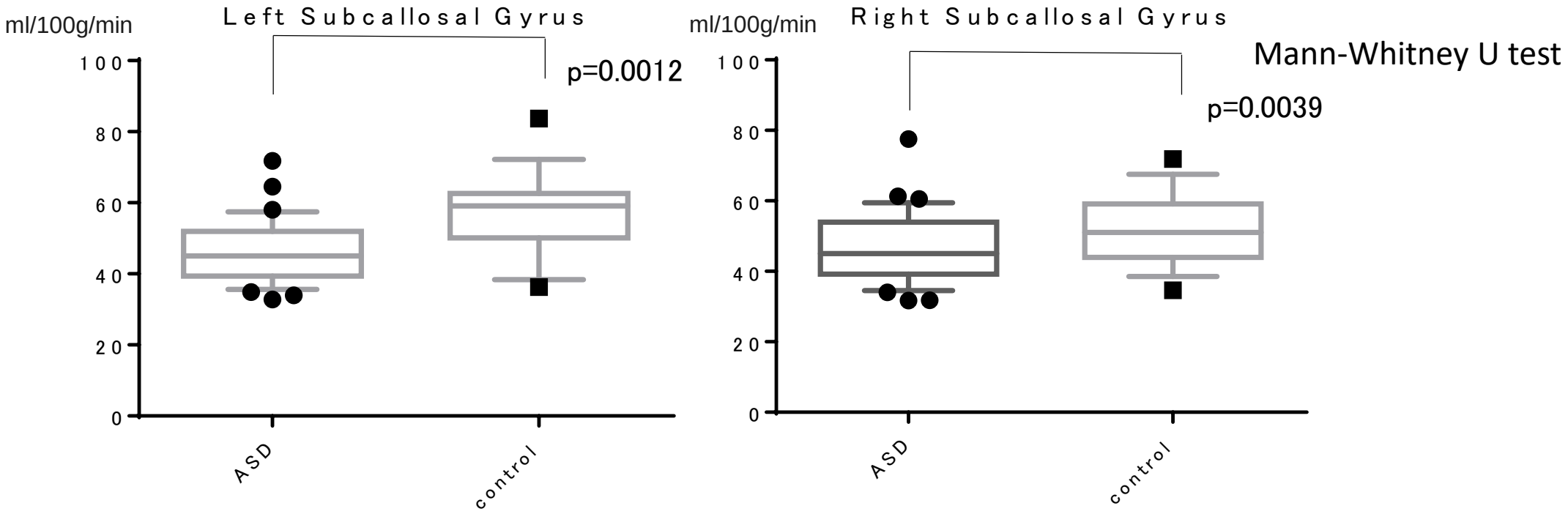
ml/100g/min
Left Subcallosal Gyrus
p=0.0012
100
80
60
40
20
0
ASD
control
ml/100g/min
Right Subcallosal Gyrus
Mann-Whitney U test
p=0.0039
100
80
60
40
20
0
ASD
control

Figure 6

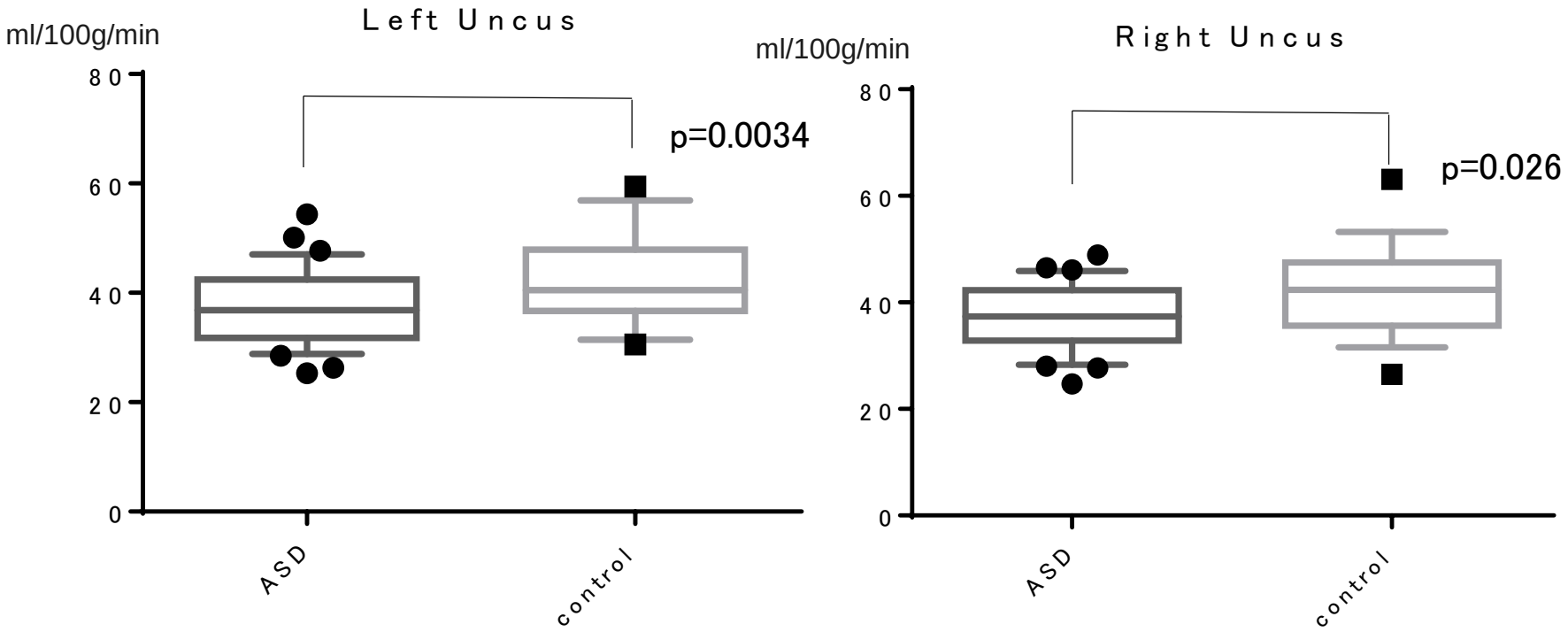
Left Uncus
ml/100g/min
80
60
40
20
0
p=0.0034
ASD
control
Right Uncus
ml/100g/min
80
60
40
20
0
p=0.026
ASD
control

Figure 7

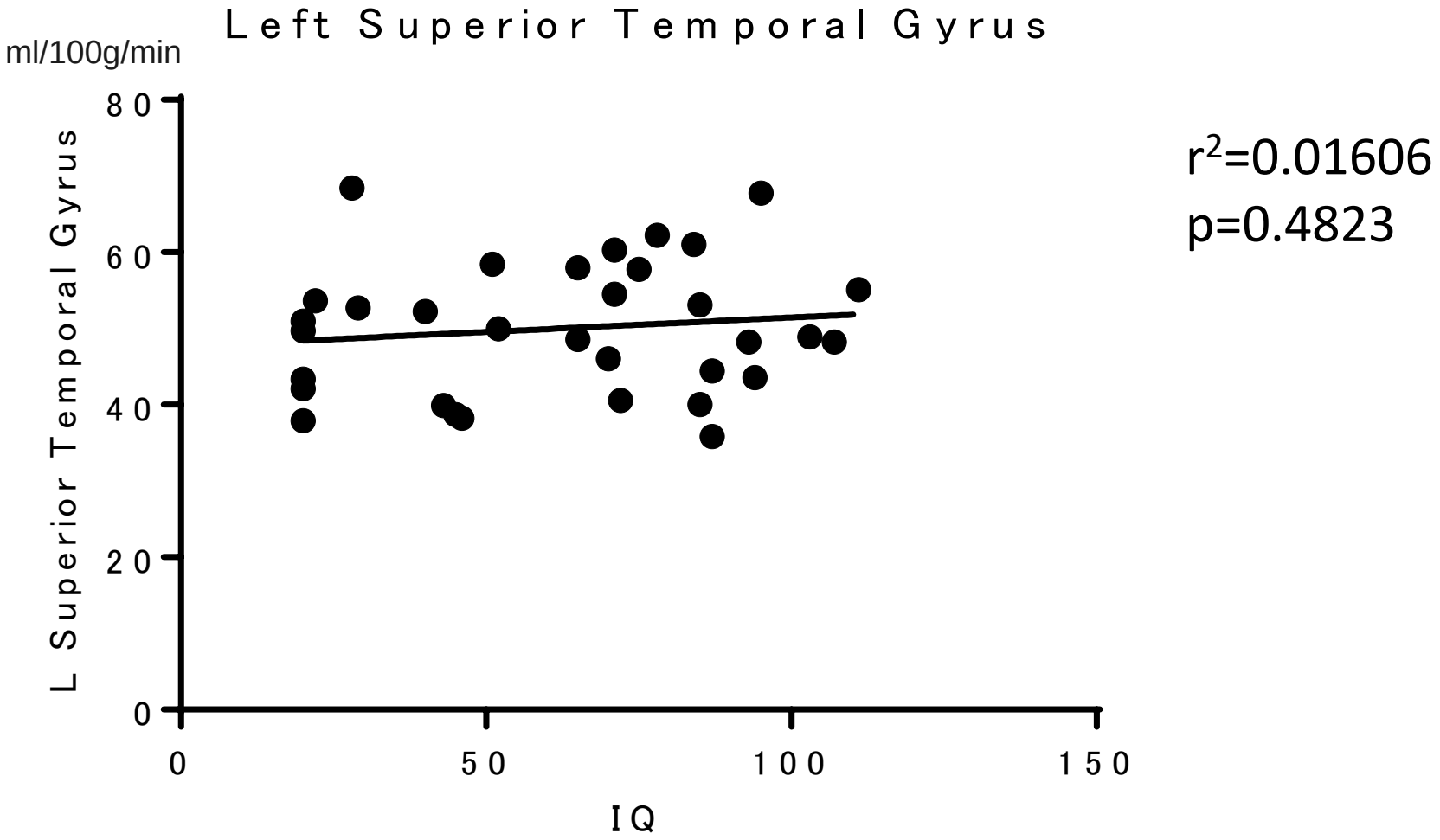
Left Superior Temporal Gyrus
ml/100g/min
L Superior Temporal Gyrus
80
60
40
20
0
0
50
100
150
IQ
r2=0.01606
p=0.4823